Anal. Chem. **2002,** *74,* 5063−5070

Shah and Sine Convolution Fourier Transform Detection for Microchannel Electrophoresis with a Charge Coupled Device

Jennifer A. McReynolds, Praneeth Edirisinghe, and Scott A. Shippy*

Department of Chemistry (M/C 111), University of Illinois Chicago, 845 West Taylor Street, Room 4500, Chicago, Illinois 60607-7061

This paper describes an improved format for Shah convolution Fourier transform (SCOFT) detection that utilizes the spatial resolution of a charge-coupled device (CCD) rather than a fixed optical mask to perform a Shah or sine convolution over a fluorescence signal. The laser-induced fluorescence from a 9-mm section of microfabricated channel is collected with a CCD at 28 Hz. Each image frame is multiplied by a convolution function to modulate the collected signal through space. Each frame is then summed to generate an intensity-versus-time data set for Fourier analysis. The fluorescence signal oscillates at a frequency dependent upon both the convolution function multiplied across each data frame and the velocity of fluorescent microspheres or a plug of fluorescent dye flowing through the channel. This SCOFT technique affords more flexibility over formats that employ a physical mask and provides data that can be optimized for signal-to-noise (S/N) or resolution information. A 1000-fold improvement in S/N is demonstrated for a plug of fluorescein dye. Detection of fluorescent beads exhibited frequency signals that were dependent upon the bead size distribution, the electric field, and the electrophoresis buffer concentration. Data are presented demonstrating the quantitation of fluorescent microspheres.

The development of miniaturized analytical separation devices by microfabrication procedures has the possibility of dramatically changing how chemical analysis is performed. The small dimensions of these devices and the possibility of including all, or most, chemical analysis functions on a chip is an exciting opportunity, but the development of optimized forms of detection is a key challenge. The low sample volumes and short path lengths tend to complicate detection; however, there have been a number of innovative developments. Detection methods have been demonstrated using analyte absorbance,[1,2] chemiluminescence,[3,4] changes in refractive index,[5] and electrochemical reactions.[6−8] By far, the most common mode of detection is laser-induced fluorescence. This is a popular technique because of its low limits of detection.[9−13]

A strategy for improving detection with cylindrical capillary electrophoresis is to use multiple points of detection or capillary imaging. The imaging of a capillary column has been used to follow the progress of separations.[14−16] Notably, a capillary image with a photodiode array utilized the individual photodiodes as independent detectors for UV absorbance at multiple points.[17] Absorbance traces for each diode were averaged for an improved S/N that was twice that theoretically expected. As an extension, the image of a capillary can be wavelength-resolved in a dimension orthogonal to the length of the capillary to attain greater chemical information. Spectrally and spatially resolved detection has been applied to both UV absorbance for capillary isoelectric focusing[18] and fluorescence imaging of a capillary.[19]

Another class of methods that have been used to improve detection for standard cylindrical capillary electrophoresis is the use of multiplex detection techniques, such as Hadamard transform[20] and correlation electrophoresis.[21−23] In both techniques,

* Corresponding author. Phone: 312-355-2426. Fax: 312-996-0431. E-mail: sshippy@uic.edu.

(1) Salimi-Moosavi, H.; Jiang, Y. T.; Lester, L.; McKinnon, G.; Harrison, D. J. *Electrophoresis* **2000**, *21*, 1291−99.
(2) Liang, Z. H.; Chiem, N.; Ocvirk, G.; Tang, T.; Fluri, K.; Harrison, D. J. *Anal. Chem.* **1996**, *68*, 1040−46.
(3) Hashimoto, M.; Tsukagoshi, K.; Nakajima, R.; Kondo, K.; Arai, A. *Chem. Lett.* **1999**, 781−82.
(4) Mangru, S. D.; Harrison, D. J. *Electrophoresis* **1998**, *19*, 2301−07.
(5) Swinney, K.; Markov, D.; Bornhop, D. J. *Anal. Chem.* **2000**, *72*, 2690−95.
(6) Fanguy, J. C.; Henry, C. S. *Electrophoresis* **2002**, *23*, 767−73.
(7) Wang, J. *Talanta* **2002**, *56*, 223−31.
(8) Woolley, A. T.; Lao, K. Q.; Glazer, A. N.; Mathies, R. A. *Anal. Chem.* **1998**, *70*, 684−88.
(9) Harrison, D. J.; Fluri, K.; Seiler, K.; Fan, Z. H.; Effenhauser, C. S.; Manz, A. *Science* **1993**, *261*, 895−97.
(10) Liu, Y. J.; Foote, R. S.; Jacobson, S. C.; Ramsey, R. S.; Ramsey, J. M. *Anal. Chem.* **2000**, *72*, 4608−13.
(11) Wallenborg, S. R.; Bailey, C. G. *Anal. Chem.* **2000**, *72*, 1872−78.
(12) Jiang, G. F.; Attiya, S.; Ocvirk, G.; Lee, W. E.; Harrison, D. J. *Bionsens. Bioelectron.* **2000**, *14*, 861−69.
(13) Ocvirk, G.; Tang, T.; Harrison, D. J. *Analyst* **1998**, *123*, 1429−34.
(14) Behnke, B.; Johansson, J.; Bayer, E.; Nilsson, S. *Electrophoresis* **2000**, *21*, 3102−08.
(15) Nilsson, H.; Wiklund, M.; Johansson, T.; Hertz, H. M.; Nilsson, S. *Electrophoresis* **2001**, *22*, 2384−90.
(16) Wu, X. Z.; Pawliszyn, J. *Electrophoresis* **2002**, *23*, 542−49.
(17) Culbertson, C. T.; Jorgenson, J. W. *J. Microcolumn Sep.* **1999**, *11*, 652−62.
(18) Wu, J. Q.; Pawliszyn, J. *Analyst* **1995**, *120*, 1567−71.
(19) Haralampus-Grynaviski, N. M.; Stimson, M. J.; Simon, J. D. *Appl. Spectrosc.* **2000**, *54*, 1727−33.
(20) Kaneta, T.; Yamaguchi, Y.; Imasaka, T. *Anal. Chem.* **1999**, *71*, 5444−46.
(21) Kuldvee, R.; Kaljurand, M.; Smit, H. C. *J. High Resolut. Chromatogr.* **1998**, *21*, 169−74.
(22) Vandermoolen, J. N.; Louwerse, D. J.; Poppe, H.; Smit, H. C. *Chromatographia* **1995**, *40*, 368−74.
(23) Vandermoolen, J. N.; Poppe, H.; Smit, H. C. *Anal. Chem.* **1997**, *69*, 4220−25.

10.1021/ac025847n CCC: $22.00
Published on Web 08/27/2002

injections are repeated in a rapid pattern. That known injection pattern is used to deconvolute the detector signal and obtain correlograms. These detection formats provide improvements in S/N at the cost of longer analysis times required for the multiple injections. The applicability of these methods to microchip electrophoresis was recently demonstrated by Fister et al., who demonstrated a S/N improvement of roughly 1 order of magnitude via correlation electrophoresis.[24]

Recently, a new form of multipoint detection, named Shah convolution Fourier transform detection, or SCOFT, was described for chip electrophoresis devices. This method utilizes a Shah convolution of the fluorescence signal during a separation. Subsequent deconvolution of the time domain signal is performed by a Fourier transform (FT). Experimentally, a length of microfabricated channel is illuminated with a continuous-wave laser through an optical mask of regularly spaced chrome regions.[25,26] The analyte fluorescence is seen only at the regions between the chrome in the mask where excitation light can be absorbed and fluorescence emitted by the analyte. This signal varies as the analyte travels down the channel at a characteristic velocity. A single-channel photomultiplier tube is used to collect all fluorescence signals emanating from all nonchrome regions through time. The FT of the time domain fluorescence signal generates a frequency spectrum corresponding to sample[25−28] or fluorescent bead[29] fluorescence oscillations. Repeated injections are compatible with SCOFT and provide an enhanced S/N.[26] SCOFT detection was also demonstrated with a new form of separation experimentation called rear analysis in which the signal from analyte bands clearing the electrophoresis channel is measured through time.[28] One of the remaining questions of the SCOFT detection technique is whether it has the ability to generate quantitative information. It has been suggested that taking the derivative of the time domain signal before performing the Fourier transform may assist with quantitation.[28]

There is one report of a FT detection technique for microchip electrophoresis utilizing a CCD.[30] Rather than illuminate the entire channel, as with SCOFT, a channel that is fabricated with a leaky waveguide is used to image the channel.[31] The leaky waveguide both propagates a fraction of the excitation light down the channel and allows some light to exit. Time-domain modulation of the signal is performed by regular, periodic injections of a fluorescent sample. Subsequent FT of each image provides the frequency spectrum with signal intensity corresponding to analyte peak-to-peak separation that is, in turn, dependent upon electrophoretic mobility.

In this paper, we present an improved format for SCOFT and demonstrate sine convolution FT detection for microchannel electrophoresis devices. This method employs a CCD to detect the laser-induced fluorescence from a length of the channel. The spatial resolution of the image data is used after fluorescence collection to modulate the signal. With the Shah function modulated signal, this system is SCOFT without physically masking the channel. A sine convolution is shown to provide an advantage over SCOFT. The multichannel detection provides greater flexibility in the application of convolution functions and allows the optimization of the frequency representation of the data. Additionally, for the first time, data are presented demonstrating that this method allows quantitation.

EXPERIMENTAL SECTION

Chemicals and Reagents. All chemicals were purchased from Sigma-Aldrich unless specified otherwise. Blue-green fluorescent, amine-modified polystyrene beads with a mean diameter of 1.01 ± 0.03 μm, as stated by the manufacturer, were obtained. Boric acid and NaOH were obtained from Fisher Scientific (Fair Lawn, NJ). The run buffer used for all experiments consisted of 20 mM borate and 0.20 mM ethylenediaminetetraacetic acid (EDTA). The borate/EDTA buffer was made by dissolving boric acid and sodium EDTA in deionized water (US Filter, Warrendale, PA) and then adjusting the solution to a pH of 9.2 with 1 M NaOH. Fluorescein was dissolved in *N*,*N*-dimethyl formamide (DMF, EM Science, Cherry Hill, NJ) and diluted with borate buffer to a concentration of 10 μM to assist in the alignment of the microchip with the CCD. For studies of instrumental performance, the fluorescein solution above was further diluted with borate/EDTA buffer to 100 nM.

Chip Electrophoresis. A commercially available glass microchip with a 100-μm double-T injection scheme was used for all experiments (Micralyne, Alberta, Canada). Prior to separations, the glass microchip was rinsed with 1 M NaOH for 5 min. This was followed by a 5-min rinse of the borate/EDTA buffer. The separation channel was then filled with the fluorescein alignment solution by vacuum. Without clearing the fluorescein from the channel, the reservoirs were replaced with the borate/EDTA buffer with the fluorescent microspheres.

The separation channel was visualized and aligned under the laser by imaging the fluorescein with the CCD detector. A potential of 3 kV was applied across the separation channel to flush the fluorescein toward the buffer waste prior to experiments. During experiments, the potential was applied at the buffer reservoir, and the data collection proceeded for the specified time period.

Potentials were applied to Pt-wire electrodes (Fisher Scientific, Pittsburgh, PA) that were inserted into buffer-filled pipet tips located in the reservoirs. Only the potentials at the buffer and waste reservoirs are controlled in experiments where beads are streamed through the channel. A LabView program created in-house was used to control the high voltage power supply (Spellman, CZE 1000R, Huntsville, NY) and a high-voltage switching system (Pickering RS232/IEEE, England). For studies of instrumental performance, the fluorescein dye solution was placed in the sample reservoir. During injection, the sample waste was grounded, the sample reservoir was held at 2 kV, and the buffer and buffer waste were held at 800 V for 10 s. During the separation, the buffer waste was grounded, the run buffer reservoir was held at 3 kV, and the sample reservoirs were held at 1 kV.

Channel Imaging and Detection. The detection system was designed with the assistance of Beam-4 ray tracing software. Unless otherwise noted, optics were purchased from Melles Griot

(24) Fister, J. C.; Jacobson, S. C.; Ramsey, J. M. *Anal. Chem.* **1999**, *71*, 4460−64.
(25) Crabtree, H. J.; Kopp, M. U.; Manz, A. *Anal. Chem.* **1999**, *71*, 2130−38.
(26) Kwok, Y. C.; Manz, A. *Analyst* **2001**, *126*, 1640−44.
(27) Kwok, Y. C.; Manz, A. *Electrophoresis* **2001**, *22*, 222−29.
(28) Kwok, Y. C.; Manz, A. *J. Chromatogr., A* **2001**, *924*, 177−86.
(29) Kwok, Y. C.; Jeffery, N. T.; Manz, A. *Anal. Chem.* **2001**, *73*, 1748−53.
(30) Holmes, R. J.; Joyce, K.; Singh, K.; Fielden, P. R. *MICRO.tec 2000: Applications, Trends and Visions*; VDE Verlag: Berlin, 2000.
(31) Hall, D. B; Yeh, C. *J. Appl. Phys.* **1973**, *44*, 2271−74.

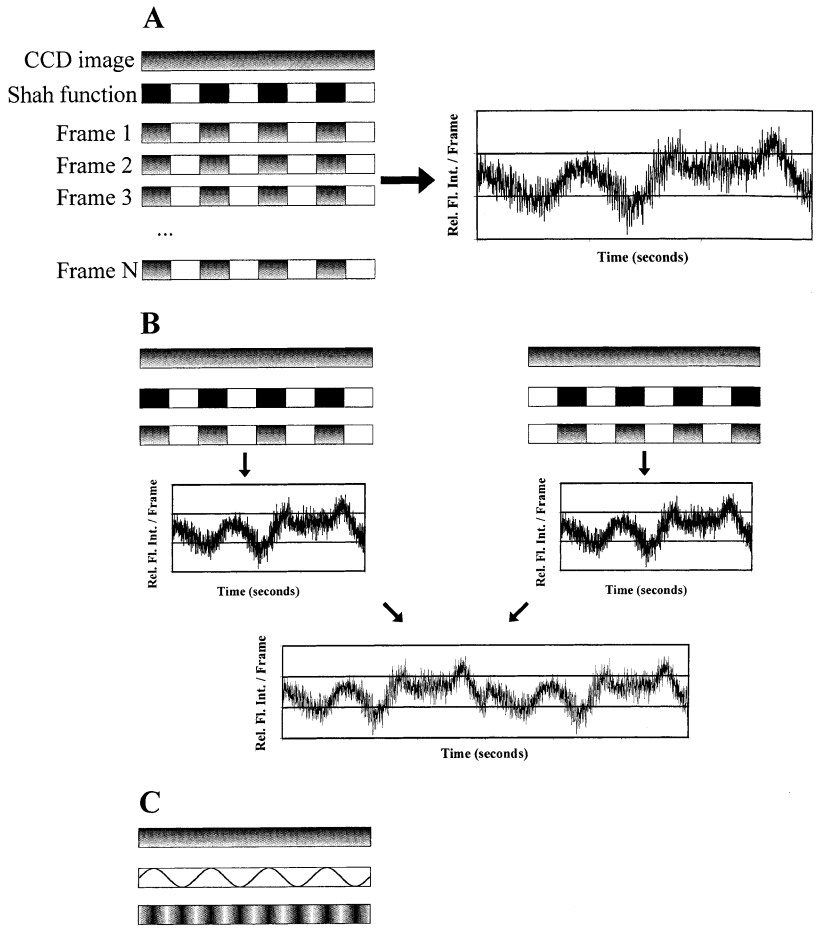

Figure 1. Schematic diagram showing the method for performing SCOFT or sine convolution FT detection without a physical mask. (A) In SCOFT, each CCD image is multiplied by a Shah function of alternating groups of 1's and 0's. The total intensity in each frame is then plotted versus frame number prior to FT analysis. (B) With an alternative to SCOFT, each CCD image is copied for the multiplication of a Shah function and its inverse. The total intensity in each frame is calculated prior to catenation of the two data sets and FT analysis. (C) In place of a Shah function, a sine wave varying from 1 to −1 is multiplied across each frame of data for sine convolution FT detection.

(Irvine, CA), and optical mountings and a pneumatically stabilized table were purchased from Newport (Irvine, CA). The 488-nm line of an Innova 90C argon ion laser (Coherent, Santa Clara, CA) was used as the excitation source. Any tube glow was eliminated by an interference band-pass filter transmitting the laser line wavelength of 488 nm (Oriel, Stratford, CT). The beam was expanded in one dimension by two cylindrical lenses and collimated in that dimension with a third cylindrical lens. A final cylindrical lens, rotated by 90°, focused the beam in the shorter dimension onto the chip. At the microchip, the laser beam was maximally located in a 9- by 0.130-mm area such that the longer axis of the beam fell along a section of the channel length near the injection T. The microchip was mounted on an optical lab jack inside an in-house-constructed, Plexiglas safety box to protect workers from high voltage. Emission from the microchannel was collected with an achromat mounted with an optimized meniscus lens. A series of 4 plano-convex lenses cemented to form two doublets were used to shape and focus the channel fluorescence image onto the detector. Scattered excitation light was removed by placing a 488-nm holographic notch filter before the detector (Kaiser Optical, Ann Arbor, MI). Detection was performed with a Spec-10:100B charge-coupled device (Roper Scientific, Trenton, NJ) having a 1340 × 100 pixel imaging array. The length of the channel formed an image on the CCD with pixel dimensions of 1200 × 30. To increase the speed of the camera read-out, the pixels across the channel width were binned into a single row and then, every 5 pixels along the channel length, were summed together before data readout. The on-chip summing produces an array size of 240 × 1 for each frame; henceforth, "pixel" refers to an element from the 240 × 1 image. The CCD was operated without a shutter at ∼28 Hz, as calculated by dividing the number of frames generated in the time required for collection. The detector was maintained at −85.0 °C with liquid nitrogen to minimize noise.

Data Manipulation. The fluorescence data was obtained with the software WinVIEW (Roper Scientific, Trenton, NJ) that was designed to operate with the CCD. Each pixel in each frame was then converted to text and exported to the MatLab software package. Although there are small fluctuations along the length of the channel due the passage of individual fluorescent microspheres, these signals are buried in the noise of the system. To convolute the data, each frame is multiplied by a function to modulate the fluorescence signal on the basis of position. There were three different modulation methods used in this report.

First, a Shah convolution similar to previous reports[25−29] was performed. A schematic diagram of the process is shown in Figure 1A. Rather than placing a physical mask over the microchip, the whole channel was imaged by the CCD. Each frame in the data set was multiplied by a Shah (or comb) function consisting of

alternating blocks of five 1's and five 0's. Thus in each frame, a regular pattern was established in which there were five pixels with fluorescent intensity followed by five pixels with zero intensity. To generate the time domain signal, the total intensity remaining in each frame was summed. A Fourier transform was then performed on this intensity-versus-time data set.

An extension of the Shah convolution takes advantage of the fact that one-half of the data set is lost in the application of the mask function and is shown schematically in Figure 1B. In this method, the Shah function is performed twice with two identical copies of the data. First, the data set is processed exactly as above. Next, the second copy of the data is multiplied by the inverse of the Shah function. In this case, the pixels set to zero in the first data set by the Shah convolution are unmodified, and pixel ranges that were unmodified in the first data set after the Shah convolution are set to zero. The intensity from each frame is summed separately for both copies of the data set. Catenating the intensity-versus-time data sets end-to-end is performed before the FT analysis.

In a third method (see Figure 1C), the CCD signal is multiplied by a sine wave that varies between 1 and −1. The number of sine wave periods multiplied across each frame was varied. As with the SCOFT methods, the intensity in each frame is summed to generate the time-domain data for FT analysis.

Visualization of the frequency domain results was performed by methods previously reported.[25] The magnitude spectrum of the data set was calculated using the relation

$$FT_{\nu,\text{magnitude}} = ((FT_{\nu,\text{real}})^2 + (FT_{\nu,\text{imaginary}})^2)^{1/2} \qquad (1)$$

and was exported to an Excel worksheet for plotting.

In experiments to study the possibility for quantitation with FT detection for microchannel electrophoresis, the derivative of the time domain signal was calculated just prior to performing the FT as described by others.[28] For these experiments, the sine-modulated, time domain data set was differentiated by subtracting frame intensities for two sequential frames through the whole data set. This derivatized result was then subjected to Fourier analysis exactly as the underivatized data.

To calculate the S/N of a cluster of peaks in the frequency spectrum, the tallest signal was used as the maximal signal before baseline subtraction. The baseline was found by averaging a 2 Hz section of the spectrum without peaks; the standard deviation of that same 2 Hz section was taken as the noise. The S/N was found by subtracting the baseline from the maximal signal and dividing by the noise. The same process was used for a single peak in the frequency domain. For single point detection, a 10-s portion of the trace was used for baseline and noise measurements.

RESULTS AND DISCUSSION

The Shah convolution Fourier transform detection method was recently described.[25] In SCOFT, the signal from a fluorescent analyte oscillates as that particle moves from masked and unmasked regions along a channel. In an unmasked region, where the channel is not covered with chrome, the analyte is excited and fluorescence emission is collected. There is no excitation or fluorescence emission of the analyte as it travels beneath the chrome-masked regions of the channel. The frequency of the signal fluctuations depends on the velocity of the analyte and is visualized by calculating the magnitude spectrum of the frequency domain data. In this work, we utilize a low-noise, multichannel detector to improve SCOFT detection and extend the technique to sine convolutions. Rather than the application of an optical mask over a length of the channel, a channel length is imaged directly, and a Shah or a sine function is multiplied across the image. In our case, the fluorescence signal is multiplied by the convolution function so that the signal varies over time as the fluorescent particles or solution plug moves through the channel (see Figure 1A). Shown in Figure 2A is a representative portion of the time domain signal that is generated after applying a Shah convolution and summing the total intensity in each frame. This time domain signal appears very similar to the data previously reported but has been obtained by post collection data manipulation rather than by physical masking.[25]

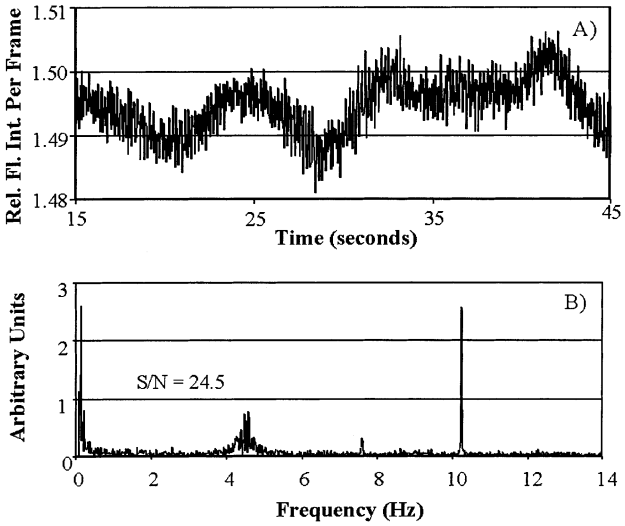

Figure 2. (A) Fluorescence data of 0.0025% fluorescent microspheres in 20 mM borate buffer with 0.2 mM EDTA and a field strength of 353 V/cm. Data were collected over 70 s with a CCD array size of 240 × 1 pixels. A 30-s portion of the data is shown. A masked/unmasked length of 10 pixels was performed, and all intensities from each frame were summed to give the two-dimension data plotted. (B) The magnitude spectrum of the SCOFT data shown in A. The signals between the frequency of 4 and 5 correlate with the migration rate of the fluorescent microspheres. The peak at 10.2 is a measurement artifact.

After taking the Fourier transform of the signal in Figure 2A, the magnitude spectrum of the frequency domain is calculated. There are two notable features of the spectrum plotted in Figure 2B. First, the frequency components due to the fluorescent beads are seen as a cluster of peaks in the 3.8−5.5 Hz frequency range. This plot is also very similar to previously published results by others;[29] however, the performance of this system represents a modest improvement in S/N. The cluster of peaks is the result of a range of sizes of the polystyrene microspheres that have slightly different electrophoretic velocities. This range of peaks is not surprising given that the manufacturer's stated variance of the diameter ±0.03 μm that corresponds to a 14% variation in bead volume. Further, there are no second harmonic peaks evident that would be seen around 8−10 Hz. The unmasked and the masked regions are defined symmetrically in our experiment by the pixels

on the camera. This result confirms what others have suggested regarding the presence of the second harmonic.[29] Second, there is a prominent peak at 10.2 Hz and a less prominent peak at 7.6 Hz seen in Figure 2B. The 10.2 Hz peak appears in all SCOFT magnitude spectra regardless of the conditions of electrophoresis, analyte concentrations, or even the presence of an electrophoresis chip. The source of this noise peak is unknown; however, the lower frequency peak is not always present, and it appears to be related to higher bead concentrations and older solutions.

Although there is another report of a FT-detection method for separations utilizing a CCD detector,[30] the format described here differs in two keys ways: The first is that a section of the channel is illuminated in the system presented here and avoids the more elaborate waveguide construction of the channel. Second, and more fundamentally, the method of modulation of the analyte signal is different. In this description, the analyte signal is modulated on the basis of its position within the channel rather than with multiple, periodic injections of sample. One benefit to the method described here is the ability to improve S/N by performing multiple injections, as has been previously demonstrated.[27] A comparison of the S/N between the two methods was not performed, because the S/N was not reported for the time-modulated method.

CCD Optimization. According to the Nyquist criterion, the highest frequency that may be seen is that at one-half the sampling rate. However, the time required to read out an image from a CCD is typically long relative to the passage of an electrophoretic or chromatographic band through a typical channel detection window. In order for a CCD to be used for SCOFT detection, the sampling rate and the illuminated length of the channel were increased. Cylindrical optics were used to increase the beam profile greatly in the direction along the length of the channel. This beam profile probes nearly 1 cm of channel. Second, the number of frames collected per second by the camera was optimized to increase the relatively slow frame rate for CCDs. The sampling frequency, or frame rate, is limited either by the time required to read out a large number of pixels or, at faster sampling rates, by the speed of a camera shutter.

First, the frame rate of the camera is increased by reducing the number of pixels that are read out. This is done by summing, or binning, the pixels across the channel width prior to readout. The binning sacrifices the spatial resolution across the channel width, but all signal that emanates from different positions across this area is still collected. In addition, binning this region prior to readout improves harvesting of low-light levels for dilute analytes. This can be explained in the following way: The predominant noise in our CCD data collection is a result of reading the charge in a pixel. When the charge from a series of pixels is added into one pixel prior to read out, there is only one read noise. This contrasts with a read noise being added to each pixel of the series when read out individually. In our case, the charge in the pixels from a row across the channel width are added together prior to readout for both higher speed and S/N.

Further, to increase the readout speed and the range of frequencies that can be detected by our system, no shutter is used in our setup. Without a shutter, any light falling on the CCD camera is collected as signal, even during readout, and introduces the possibility of image blurring, or more appropriately with our system, stray light noise. However, the fact that the frame rate can be increased dramatically minimizes the possibility of blurring the data. This is because the fast frame rate decreases the likelihood of stray signal photons collecting above the level of the noise during any one read.

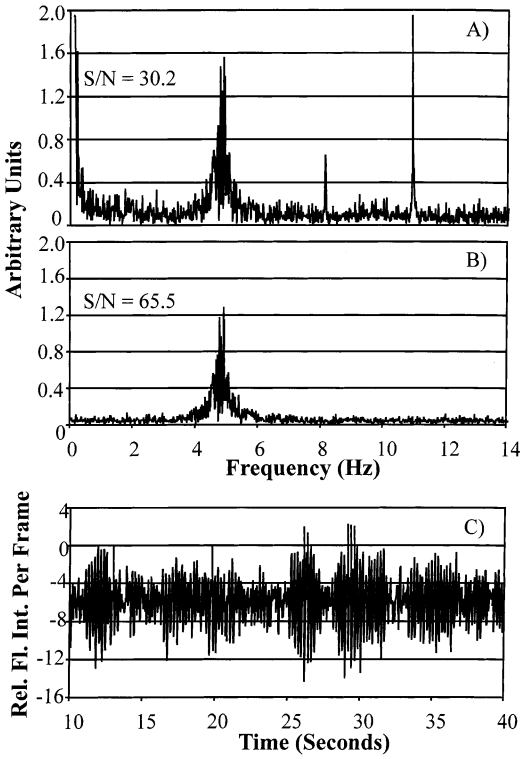

Figure 3. Comparison of the same data set and instrumental settings as in Figure 2 with different post collection analysis performed: (A) SCOFT utilizing all collected data by performing two convolutions with a masked/unmasked length of 10 pixels, (B) magnitude spectrum of sine convolution FT analysis on same data set with 10 pixels/period, and (C) a 30-s portion of the time domain data of B after the sine convolution.

Alternate Modulation of Signal over the Pixel Space. The modest improvement in S/N seen with the SCOFT format presented here may be a result of several factors. First, our data have not been filtered for optimization of signal. The use of filtering or smoothing routines with the raw data before calculating the FT may enhance the performance of this method. Further, the Shah convolution process generates a data set that contains one-half of the signal that was collected by the detector. The other half of the data was set to zero. In Figure 3A, we demonstrate an alternative presentation of the data from Figure 2 that utilizes all the data collected. In this method, the Shah convolution has been applied to the data set twice such that alternate halves of the data set have been set to zero. These two Shah-modulated data sets are catenated and processed further as one. It is clear from the data that there is another modest improvement in S/N over the original SCOFT method, as would be expected.

Another possible improvement addresses the possibility that the Shah convolution itself might degrade the S/N because of the masking function that employs a step change between passing signal/no signal. Similar to the methods for apodization used to avoid side lobes in FT nuclear magnetic resonance spectra, the use of a smooth convolution function between the signal/no signal

regions in each frame may provide an enhancement in the S/N in the magnitude spectrum. In Figure 3B and C, we demonstrate that the use of a sine function in place of a Shah convolution improves the S/N for our system. There are a number of striking features of this presentation of the data. First, the frequency domain shows an enhanced S/N and that the low frequency noise component is nearly eliminated. In comparison to our SCOFT detection, there is an improvement of >2 and an overall improvement of >5.4 over previous reports.[29] Surprisingly, the noise peak at 10.2 Hz is not seen. The time domain signal shown in Figure 3C appears to be more regular than that for SCOFT (Figure 2A). Importantly, the whole data set is utilized with a sine modulation of the signal across the channel length. Pixels are multiplied by sine values ranging from 1 to −1, and relatively few data points are set to zero, as compared to SCOFT. The maxima and minima of the sine wave can be thought of as a series of unmasked and masked regions, respectively. The frequency observed after FT analysis, then, relates to the distance the particle traveled from the positive maximum of the sine wave to that of the next period. For instance, the fundamental frequency is the same for that of the sine-modulated data with 10 pixels set between sine wave positive maxima (Figure 3B) and the Shah modulated data (Figure 2B), with 10 pixels set for the center of one "window" to the next. Finally, it is also important to point out that all collected data points are used in the FT analysis for the whole time that the bead is in the imaged section of the channel and likely contributes to the higher signals seen with this new FT detection format.

With the fluorescent microspheres, there is a difficulty in comparing the performance of the detection schemes, because individual beads may be detectable. To more quantitatively compare the instrumental performance of this method to single-point detection and to previous reports, 100 nM fluorescein dye was used as the analyte for a series of injections. In Figure 4, we present the data from a representative injection of fluorescein in three formats: (a) the sine-modulated intensity data (frame intensity versus time), (b) the magnitude spectrum of the FT of sine-modulated data, and (c) the magnitude spectrum of the SCOFT format. Different from continuous streaming of beads, the fluorescein plug flows through the illuminated channel region for ~8 s (Figure 4A). The plug residence is clearly seen as intensity fluctuations in the sine-modulated data. The FT of the sine convolution and SCOFT signal (Figure 4B,C) shows the frequency components of the data that, in this case, corresponds only to the fluorescein plug. The fluorescein frequency is seen clearly at 0.86 Hz. The same data set was used for comparison to single-point detection. To obtain the single-point detection electropherogram, the total signal in the first four pixels of the illuminated region of each frame were summed and plotted versus time (data not shown). Table 1 compares the performance of the various formats of detection presented here. From the data presented in this work, it is clear that both the SCOFT and sine convolution formats perform better than the single-point detection. In addition, the sine convolution format provides a significant advantage in S/N over the SCOFT format; however, the relative error is also higher. In comparison to previously reported results, our SCOFT method provides an improvement of >3 orders of magnitude. This dramatic improvement is likely due to the lower noise associated with the CCD detector in comparison to a photomultiplier tube.

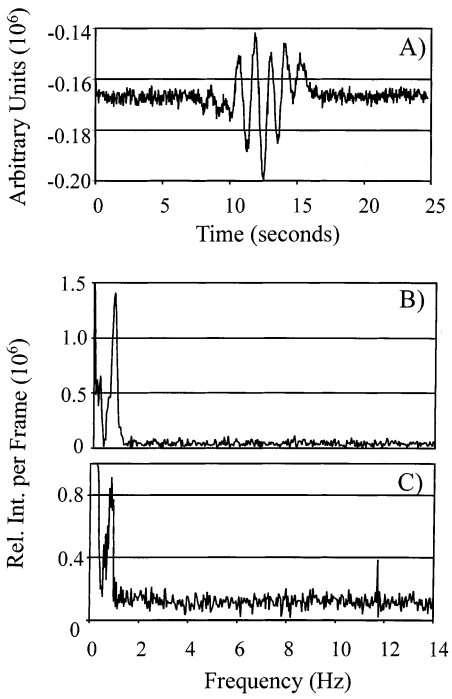

Figure 4. Three different representations of the same 100 nM fluorescein separation. The run buffer was 20 mM borate buffer, pH 9.2, with 0.2 mM EDTA, and the separation field strength was 352 V/cm. (A) Time domain data after sine modulation. (B) Magnitude spectrum of the data presented (A) after FT analysis. (C) Magnitude spectrum of the data following SCOFT (the time domain data is not shown.)

Table 1. Detector Performance Comparisons for Single Injections of 100 nM Fluorescein Dye

av ($n = 3$)	S/N	std dev
single-point detection	9.9	2.1
SCOFT		
spatially resolved detection	18.8	0.8
sine convolution FT	51.5	6.0

Velocity Measurement of Microspheres. To confirm that the source of the cluster of peaks seen with our sine convolution FT detection is, in fact, the fluorescent microspheres, a series of experiments were performed in which the electric field and the electrophoresis buffer concentration were varied. The only difference noted between magnitude spectra is the movement of the cluster of peaks (data not shown); therefore, in Figure 5, the fundamental peak in these experiments is plotted versus the field strength. There is a linear dependence on the observed peak frequency with respect to electric field strength, as expected. Because the velocity of any particle directly depends on the magnitude of the electric field in electrophoresis, the results suggest that the peak assignment is correct. It is notable that at the lower electrolyte concentrations, the frequency of the bead signal (and hence, velocity) increased.

When the length of the channel that corresponds to each pixel is known, an analyte velocity can be directly calculated. The channel length corresponding to each pixel in our system was calculated separately by measuring the number of pixels between six microfabricated channels whose separation is known and each of which is filled with a fluorescein solution. This capillary array

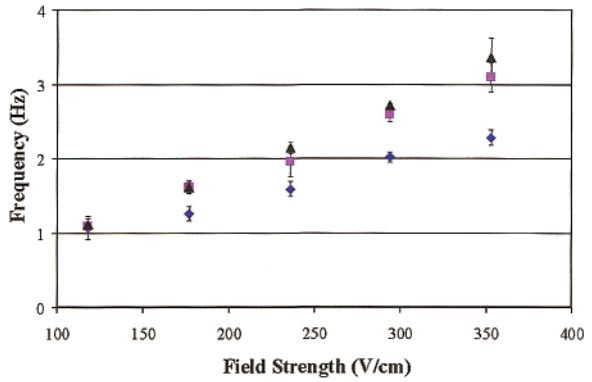

Figure 5. Effect of run buffer concentration versus increasing field strength on a sine-modulated data set with 10 pixel/period: 20 mM borate buffer (▲), 40 mM borate buffer (■), and 80 mM borate buffer (◆). All instrumental settings are the same as in Figure 2.

was oriented orthogonally to the long direction of the camera for measurement of the distance per pixel (data not shown), which was found to be 33 ± 2 μm of channel length/pixel. With the sine wave frequency set to 10 pixels between positive maxima, the total distance between expected fluorescence signal maxima is 330 μm. Then, for a 2 Hz signal, the measured linear velocity of a 1-μm bead is ~660 μm/sec. This compares favorably to other published results.[29] This also further confirms the assignment of the cluster of peaks as the fluorescent beads.

Application of Different Sine Convolutions. Because the entire length of the channel is imaged without a physical mask, the convolution function is easily varied in the data processing software. In Figure 6, the magnitude spectra of one data set are presented following sine modulation by a number of different pixels/wave periods. At a low number of pixels/period, the peak distribution is found at relatively high frequencies and is limited by the sampling rate. As the pixels/period is increased (Figure 6B−D), the frequency of the fluorescent microsphere signal decreases. This is expected, because the distance that a microsphere must travel between sine wave maxima is also increased with a higher number of pixels/period.

This ability to reprocess data provides the possibility of optimizing the modulation to obtain different information. For instance, to obtain a fine resolution of the distribution of the beads, Figure 6A would be the first choice, given the wide frequency distribution of the signal. Because the signal corresponding to beads is spread over a wide frequency range, the S/N is the lowest of all sine convolutions. Alternately, the S/N of the analysis is shown to be improved by increasing the pixels/wave period. The microsphere signal is higher, because it is spread over a decreased frequency range. A larger range of component velocities can be detected with this format, because the sine modulation can be modified to bring an analyte velocity within the detectable frequency range. Both slower and faster components could be resolved by processing the data with different sine convolutions. Additionally, the ability to select the signal frequency range is a useful feature for the avoidance of any noise such as low frequencies.

A closer examination of the data in Figure 6 shows that the peak profile also varies as the number of pixels/period is increased. This difference may be due to the different number of data points that define each distribution. For instance, the peak

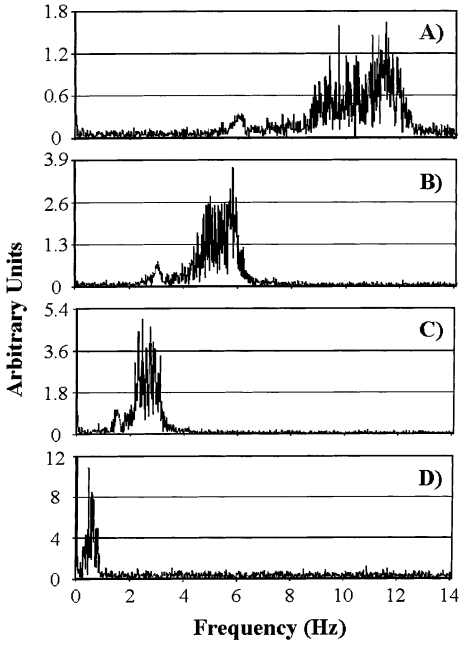

Figure 6. FT analysis of a data set that illustrates the effect of increasing the number of pixels/period during sine modulation. The same data set was used for each plot. All instrumental settings are the same as in Figure 2, except that the bead concentration was 0.025% operated at a field strength of 588 V/cm. Number of pixels per period used for the sine modulation: (A) 5, (B) 10, (C) 20, and (D) 100.

region of 11.0−11.8 Hz depicted in Figure 6A is defined by 54 data points, whereas there are only 4 in the corresponding region in Figure 6D (0.55−0.59 Hz.) Additionally, there is a different amount of noise present in each peak distribution. The noise in the time domain is distributed evenly over all data points in the frequency domain, so there is more noise with a larger number of data points (and a lower S/N). Although the peak profiles do differ in the magnitude spectra, data can be processed with the same modulation function for comparisons between data sets.

Particle Quantitation. Although the detection of particle velocities is useful, the method would ideally also allow quantitation. A series of different bead concentrations were electrophoresed through the channel for a set time to determine whether quantitative information is available with SCOFT or sine convolution FT detection methods. The data collected for Figure 7 was processed in three different ways: In one, the S/N of the tallest frequency was calculated from the magnitude spectrum from the SCOFT detection. For comparison, the S/N was calculated from the magnitude spectrum of the same data that was sine-modulated. In the third method, the S/N was calculated from the magnitude spectrum of sine-modulated data in which the time domain signal was differentiated immediately prior to the FT analysis. Kwok and co-workers have proposed that taking the derivative of the data before the Fourier transform, SCODFT, may allow quantitative assessment in the frequency domain.[28] In all cases, 50 pixels/period or a 50-pixel length for masked/unmasked regions were used in order to compare the signal intensities.

First, the S/N was plotted versus the bead concentration (see inset of Figure 7). All methods used to process the data show a relationship between signal and concentration that appears to be logarithmic. This result is surprising, because there should be a

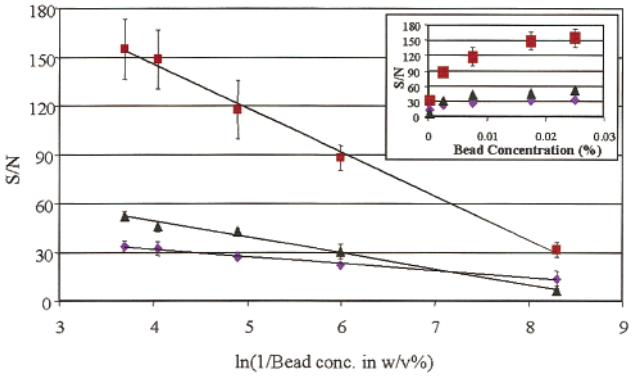

Figure 7. Plot of S/N versus the natural log of the inverse of the fundamental frequency at different fluorescent bead concentrations performed by FT analysis. The line is the result of a linear regression. The inset shows the same data sets are used to plot the S/N of the fundamental frequency versus increasing bead concentration. For the sine convolution data, the number of pixels/period was 50, and for the SCOFT experiments, the length of the masked/unmasked region was 50 pixels. Instrumental settings were the same as in Figure 2. Symbols are for sine convolution FT analysis (■), differentiation of the sine convolution FT analysis (◆), and SCOFT analysis (▲).

linear increase in the signal as a result of more beads flowing through the channel. The slower increase in S/N with higher bead concentrations appears to be the result of higher noise. Possible sources for this increased noise may be the higher fluorescence flux at higher bead concentrations that increases blurring of the channel image or higher shot noise at higher signal intensities.

To fit the data to a straight line, the S/N was then plotted versus the natural log of the inverse of the percentage of the beads in solution, because the data appears logarithmic. The plots in Figure 7 show the linear relationship. Notably, all of the different data treatments demonstrate clear linear trends in S/N. Most striking is the dramatically higher sensitivity of the sine-modulated signal versus the differentiated sine convolution FT and the SCOFT analysis. The high signal does appear to come at the cost of higher error, however. It was observed that the noise, the standard deviation of the signal from a 2 Hz-long part of the frequency spectrum without peaks, also varies with the signal. The regression of the S/N from the magnitude spectrum of the sine-modulated data was used to calculate a limit of detection (S/N = 3) of 0.000 09% beads for a 70-s integration of signal. Using eq 2,

$$\text{no. beads/mL} = \frac{0.06C \times 10^{12}}{\rho\pi\phi^3} \qquad (2)$$

where C is the solution percentage of beads, ρ is the density of the polystyrene polymer, and ϕ is the average diameter of the beads in micrometers. The approximate number of microspheres at the detection limit is 1.6×10^6 beads/mL. This system's performance at 0.002% beads is better than previous reports by a factor of 5.4.[29] Importantly, these data demonstrate that particle quantitation is possible.

Further, it may be instructive to consider the significance of the S/N for a given frequency. The intensity at each frequency is a measure of the amount of that frequency in the time domain signal. As such, a longer integration time may result in a higher peak intensity, as long as the noise adds more slowly than the signal. Interestingly, Kwok et al. described no enhancement due to an increase in integration time[29] that could be the result of an equal increase of both noise and signal. In addition to increasing the integration time, signal may be enhanced by the presence of more fluorescence oscillations during the sample period. Our data supports this conclusion, because there is a higher signal with progressively higher percentages of beads flowing through the channel. Kwok and Manz also demonstrated this finding with multiple sample plug injections.[27] Importantly, there is a linear relationship between signal and the natural log of the inverse of the bead concentration over the three decades of bead concentrations tested and for all FT transform methods.

CONCLUSIONS

This new detection format for Shah and sine convolution FT detection offers some advantages over previous reports. Most notably, the greater flexibility of the system for data analysis after collection provides the ability to select a signal frequency range for the avoidance of any noise and to optimize the peak resolution and the S/N desired. The ability to use this method for quantitation of particles has been demonstrated with this detection format for the first time. Future developments would include the exploration of higher velocity signals, including analyte bands in electrophoresis. This pixel space modulation will be expanded to other functions and may offer other benefits in analysis including S/N improvement or peak resolution.

ACKNOWLEDGMENT

The authors acknowledge the financial support of the University of Illinois Chicago and the UIC Campus Research Board for financial support.

Received for review June 10, 2002. Accepted July 25, 2002.

AC025847N